DC spin generation by junctions with AC driven spin-orbit interaction

Jonson, Mats; Shekhter, Robert I.; Entin-Wohlman, Ora; Aharony, Amnon; Park, Hee-Chul; Radić, Danko

Source / Izvornik: **Physical Review B, 2019, 100**

Journal article, Published version
Rad u časopisu, Objavljena verzija rada (izdavačev PDF)

https://doi.org/10.1103/PhysRevB.100.115406

Permanent link / Trajna poveznica: https://urn.nsk.hr/urn:nbn:hr:217:294775

DC spin generation by junctions with AC driven spin-orbit interaction

M. Jonson,[1] R. I. Shekhter,[1] O. Entin-Wohlman,[2] A. Aharony,[2] H. C. Park,[3] and D. Radić[4]
[1]*Department of Physics, University of Gothenburg, SE-41296 Göteborg, Sweden*
[2]*Raymond and Beverly Sackler School of Physics and Astronomy, Tel Aviv University, Tel Aviv 69978, Israel*
[3]*Center for Theoretical Physics of Complex Systems, Institute for Basic Science, Daejeon 34051, Republic of Korea*
[4]*Department of Physics, Faculty of Science, University of Zagreb, Bijenička 32, Zagreb 10000, Croatia*

(Received 14 March 2019; revised manuscript received 20 June 2019; published 4 September 2019)

An unbiased one-dimensional weak link between two terminals, subjected to the Rashba spin-orbit interaction caused by an AC electric field which rotates periodically in the plane perpendicular to the link, is shown to inject spin-polarized electrons into the terminals. The injected spin polarization has a DC component along the link and a rotating transverse component in the perpendicular plane. In the low-rotation-frequency regime, these polarization components are proportional to the frequency. The DC component of the polarization vanishes for a linearly polarized electric field.

DOI: 10.1103/PhysRevB.100.115406

I. INTRODUCTION

Spintronics takes advantage of electronic spins in designing a variety of applications, including giant magnetoresistance sensing, quantum computing, and quantum-information processing [1–3]. A promising approach for the latter exploits mobile qubits, which carry the quantum information via the spin polarization of moving electrons. The spins of mobile electrons can be manipulated by the spin-orbit interaction (SOI), which causes the spin of an electron moving through a spin-orbit-active material (e.g., a semiconductor heterostructure [4]) to rotate around an effective magnetic field [5,6]. In the particular case of the Rashba SOI [7], the magnitude and direction of this field can be tuned by gate voltages [8–11]. The Rashba SOI is mostly significant at surfaces and interfaces because of strong internal uncompensated atomic electric fields perpendicular to the surface/interface. These occur since the (weaker) surface/interface potential breaks the symmetry of the atomic orbitals there, so that the corresponding strong atomic fields no longer cancel as they do in the bulk. An electric field induced by external gates can then modulate the resulting SOI to a certain extent by changing the degree of orbital asymmetry.

One aim of spintronics is to build logic devices [3], which produce spin-polarized electrons, so that one can use their electronic spinors as qubits. In the simplest device, electrons move between two large electronic reservoirs via a nanoscale quantum network. For this two-terminal case, the time-independent SOI that obeys time-reversal symmetry cannot generate spin splitting [12]. Time-reversal symmetry can be broken by applying a magnetic field, either via a magnetic flux, which penetrates SOI-active loops of Aharonov-Bohm interferometers [13–15], or by a Zeeman magnetic field [16,17]. Alternatives utilize ferromagnetic terminals [18,19].

Here we explore yet another means to break time-reversal symmetry, exploiting time-dependent Hamiltonians. Several papers proposed the generation of spin splitting by quantum spin pumping, in which different terms in the system's Hamiltonian vary slowly periodically with time. Some of these require DC or AC magnetic fields [20–22]. Here we concentrate on all-electrical devices, which pump polarized electrons. One such device used an out-of-phase oscillation of the heights of the barriers representing the contacts between a planar quantum dot and the two leads to yield a spin current with polarization perpendicular to the plane [23]. Alternatively, polarized spins were created by periodic variations of one barrier height and of the strength of a uniaxial SOI (induced by an electric field perpendicular to the quantum dot's plane) [24]. In a third example, a one-dimensional wire was split into two regions, with two differently oriented SOI-generating electric fields which oscillate periodically with time [25]. In these examples, the two gate voltages act at different locations of the system, and the calculation yields only the average spin current, integrated over a period of the oscillation.

Below we consider the possibility to activate spin splitting via weak links (also called "junctions") by breaking time-reversal symmetry with an AC Rashba SOI created by an electric field that rotates slowly with frequency Ω perpendicular to the (one-dimensional) weak link. A rotating field can result from two external fields along perpendicular directions, which are normal to a thin cylindrical wire. When the two fields oscillate periodically with time, with a phase difference of $\pi/2$, the resultant vector rotates around the wire. Such fields can be produced by gate voltages $V_y(t)$ and $V_z(t)$, applied to electrodes as in Fig. 1(a) [26]. They can also be generated by rotating a bent wire periodically under a uniform electric field [27] or from a circularly polarized electromagnetic field. Even in the absence of a bias we find that a *time-independent* DC flow, towards both terminals, of electrons whose spins are polarized parallel to the junction's direction is created in the junction (as indicated by arrows in the weak link shown in Fig. 1). In addition, the time dependence of the SOI in the weak link gives rise to transverse components of the polarization, which rotate in the plane perpendicular to the junction parallel to the effective SOI magnetic field. These transverse components vanish upon averaging over a period and thus would not appear in the "standard" spin-pumping approach.

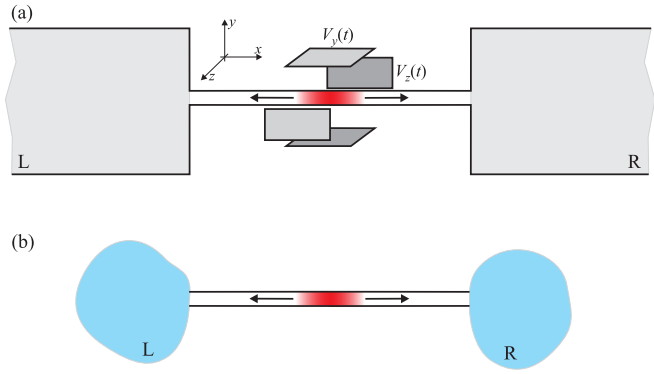

FIG. 1. Schematic visualizations of devices proposed in the text. (a) A spin-orbit-active weak link connects two contacts, L and R, to form a closed circuit [28]. The time-dependent spin-orbit interaction is generated by two perpendicular gates, whose potentials $V_y(t)$ and $V_z(t)$ oscillate slowly in time with frequency Ω. The arrows within the weak link indicate the directions in which polarized electron spins are flowing. (b) An open-circuit version of (a) where spin is accumulated in two terminals, leading to a magnetization that can be measured.

We analyze in detail the case of a circularly polarized electric field and then extend the discussion to allow for an elliptic variation of the field, all the way to the limit of a longitudinal uniaxial oscillation, where the DC spin polarization is found to vanish.

Our model is described in Sec. II, where we also give general expressions for the charge and spin currents. A detailed derivation of these currents is presented in Appendix A. Sections III and IV then present explicit results for these currents for circularly and elliptically rotating electric fields. Technical details of these calculations appear in Appendix B. Our conclusions are then discussed in Sec. V.

II. MODEL AND CURRENTS

Electronic transport through a spin-orbit-active weak link can be analyzed within the framework of an effective tunneling Hamiltonian,

$$\mathcal{H}_{\rm tun}(t) = \sum_{k,p}\sum_{\sigma,\sigma'}\{[W_{LR}(t)]_{\sigma\sigma'}c^\dagger_{k\sigma}c_{p\sigma'} + \text{H.c.}\}, \tag{1}$$

where $c^\dagger_{k\sigma}$ ($c_{k\sigma}$) creates (annihilates) an electron of wave vector k and spin index σ in the left electrode [29]; the wave vectors on the right are denoted by p. The tunneling amplitude $W_{LR}(t)$ from right to left is a (2×2) matrix in spin space, independent of the wave vectors; that is, it is approximated by its value at the Fermi energy. For the Rashba SOI, this tunneling amplitude has the form

$$W_{LR}(t) = W_0\exp[i\boldsymbol{\varphi}_{\rm AC}(t)], \tag{2}$$

where W_0 sets the magnitude of the tunnel coupling (in units of energy) and the Aharonov-Casher [30,31] phase operator is

$$\boldsymbol{\varphi}_{\rm AC}(t) = k_{\rm so}d[\hat{\mathbf{x}}\times\hat{\mathbf{n}}(t)]\cdot\boldsymbol{\sigma}. \tag{3}$$

Here $\boldsymbol{\sigma} = (\sigma_x,\sigma_y,\sigma_z)$ is the vector of the Pauli matrices, the unit vector $\hat{\mathbf{x}}$ is along the weak link whose length is d, and $k_{\rm so}$ is the strength of the SOI (in units of inverse length), resulting from an electric field directed along $\hat{\mathbf{n}}(t)$; its explicit form is specified below.

Equation (3) was derived in Ref. [32] for a time-independent SOI, $\hat{\mathbf{n}}(t) = \hat{\mathbf{n}}$. A generalization to the time-dependent case considered here would, in principle, require an analysis of electron tunneling through a device, which includes the nontrivial dynamics of the SOI. One would expect such an analysis to lead to a nonlocal temporal relation between the Aharonov-Casher phase and the electric field direction. In the present paper we divide the calculation into two steps: in the first step, we neglect this nontrivial dynamics and treat the time t in Eq. (3) as a parameter. In particular, we expect this approximation to be valid when the time dependence of the SOI is slower than all other timescales in the system. Assuming that the electric field rotates with frequency Ω, the result may be justified for $\Omega\tau \ll 1$, where τ is the electron dwell time before the electron escapes from the weak link to an adjacent reservoir (to be estimated below). In the second step we use a full time-dependent perturbation expansion in the tunneling matrix elements $W_{LR}(t)$.

The entire tunnel junction is modeled by the Hamiltonian

$$\mathcal{H} = \mathcal{H}_{\rm leads} + \mathcal{H}_{\rm tun}(t), \tag{4}$$

where the first term describes the nonpolarized (free-electron) leads

$$\mathcal{H}_{\rm leads} = \sum_{k,\sigma}\epsilon_k c^\dagger_{k\sigma}c_{k\sigma} + \sum_{p,\sigma}\epsilon_p c^\dagger_{p\sigma}c_{p\sigma} \tag{5}$$

and $\epsilon_{k(p)}$ is the single-electron energy in the left (right) lead.

The rates of change of the particle number and of the magnetization in the left lead are determined by the rate matrix

$$[R_L]_{\sigma\sigma'}(t) \equiv \frac{d}{dt}\sum_k\langle c^\dagger_{k\sigma}(t)c_{k\sigma'}(t)\rangle, \tag{6}$$

where angular brackets indicate quantum averaging. Specifically, the particle current into the left electrode $I_L(t)$ is the rate of change of the particle occupation there,

$$I_L(t) = \frac{d}{dt}\sum_\sigma\sum_k\langle c^\dagger_{k\sigma}(t)c_{k\sigma}(t)\rangle \equiv \sum_\sigma[R_L(t)]_{\sigma\sigma}, \tag{7}$$

while the rate of change of the total spin in the left terminal, and hence the spin current into that terminal, is $(\hbar/2)\dot{\mathbf{M}}_L$, with

$$\dot{\mathbf{M}}_L = \frac{d}{dt}\sum_{\sigma,\sigma'}\sum_k\langle c^\dagger_{k\sigma}(t)\boldsymbol{\sigma}_{\sigma\sigma'}c_{k\sigma'}(t)\rangle \equiv \sum_{\sigma,\sigma'}[R(t)]_{\sigma\sigma'}\boldsymbol{\sigma}_{\sigma\sigma'}. \tag{8}$$

It follows that the rate of change of magnetization in the left lead is $(g\mu_B/2)\dot{\mathbf{M}}_L$ (g is the g factor of the electrodes, and $\mu_{\rm B}$ is the Bohr magneton; see Sec. V).

As detailed in Appendix A [see Eq. (A3)], perturbation theory to second order in the tunneling amplitude gives ($\hbar = 1$, $\eta\to 0^+$)

$$[R_L]_{\sigma\sigma'}(t) = \sum_{k,p}[f_R(\epsilon_p) - f_L(\epsilon_k)]\int_{-\infty}^{t}dt_1 e^{\eta t_1} \times (e^{i(\epsilon_k-\epsilon_p)(t-t_1)}[W_{LR}(t)W^\dagger_{LR}(t_1)]_{\sigma'\sigma} + \text{H.c.}). \tag{9}$$

Here

$$f_{L(R)}(\epsilon_{k(p)}) = \{\exp[(\epsilon_{k(p)} - \mu_{L(R)})/(k_B T)] + 1\}^{-1} \quad (10)$$

is the equilibrium Fermi function in the left (right) lead, whose chemical potential is $\mu_{L(R)}$.

III. CIRCULARLY ROTATING FIELD

For a circularly polarized electric field $\mathbf{n}(t) = \cos(\Omega t)\hat{\mathbf{z}} - \sin(\Omega t)\hat{\mathbf{y}}$, and thus, the tunneling amplitude is

$$W_{LR}(t) = W_0[\cos(k_{so}d) + i\sin(k_{so}d)\boldsymbol{\sigma}\cdot\hat{\mathbf{v}}(t)], \quad (11)$$

where

$$\hat{\mathbf{v}}(t) = [0, \cos(\Omega t), \sin(\Omega t)] \quad (12)$$

lies in the y-z plane as well. Consequently,

$$\begin{aligned} &W_{LR}(t)W_{LR}^{\dagger}(t_1)/|W_0|^2 \\ &= \cos^2(k_{so}d) + \sin^2(k_{so}d)\hat{\mathbf{v}}(t)\cdot\hat{\mathbf{v}}(t_1) \\ &\quad + i\boldsymbol{\sigma}\cdot\{\cos(k_{so}d)\sin(k_{so}d)[\hat{\mathbf{v}}(t) - \hat{\mathbf{v}}(t_1)] \\ &\quad + \sin^2(k_{so}d)\hat{\mathbf{v}}(t)\times\hat{\mathbf{v}}(t_1)\}. \end{aligned} \quad (13)$$

The particle current, Eq. (7), requires the trace of the matrix $R_L(t)$, hence [see Eq. (9)] the trace of $W_{LR}(t)W_{LR}^{\dagger}(t_1)$. As shown in Appendix B, this trace depends only on $(t - t_1)$. Assuming also that the densities of states in the terminals are energy independent [33], $\mathcal{N}_{L(R)}(\epsilon) = \mathcal{N}_{L(R)}(\epsilon_F) \equiv \mathcal{N}_{L(R)}$ (wide-band approximation), and if $\mu_R - \mu_L = eV$, then in the limit of low bias voltage V and low temperature Eq. (B4) yields

$$I_L = GV/e, \quad G = 4\pi^2|W_0|^2\mathcal{N}_L\mathcal{N}_R G_0, \quad (14)$$

where $G_0 = e^2/(\pi\hbar)$ is the quantum of conductance. Clearly, the particle current is not affected by the spin-orbit interaction.

The current into the right terminal I_R is (see Appendix B) $I_R = -I_L$, demonstrating that particle number is conserved in the junction. For the spin currents, however, there is no such conservation law, and in fact, spin-flip transitions generated by the SOI in the weak link may result in the accumulation of spin polarization. Indeed, as seen in Eqs. (15) and (17) below for the spin polarization in the left lead, interchanging L with R in each of them to obtain the spin polarization in the right one leaves them intact, $\dot{\mathbf{M}}_L(t) = \dot{\mathbf{M}}_R(t)$; the total spin is not conserved, and the junction injects the same amount of spin polarization into the two leads, even in the absence of any bias voltage.

From Eqs. (8) and (9), the spin current requires the trace of $\boldsymbol{\sigma}W_{LR}(t)W_{LR}^{\dagger}(t_1)$. Equation (B5) then implies that (with the same assumptions as above) the x component of the spin-polarization flow is proportional to

$$\dot{M}_{L,x} = (G/G_0)\mathcal{F}(\Omega)\sin^2(k_{so}d), \quad (15)$$

where

$$\begin{aligned} \mathcal{F}(\Omega) = \int \frac{d\omega d\omega'}{2\pi}[f_L(\omega) - f_R(\omega')] \\ \times[\delta(\omega - \omega' + \Omega) - \delta(\omega - \omega' - \Omega)]. \end{aligned} \quad (16)$$

Interestingly, the x component of the injected spin polarization is time independent; the AC electric field yields a DC polarization in the leads, parallel to the junction. At small Ω, the difference of the two δ functions in Eq. (16) is proportional to Ω, indicating inelastic processes: electrons exchange photons of energy Ω with the electric field and, accordingly, flip their spins. For instance, at zero temperature only absorption processes are allowed in an unbiased junction; these lead to pumping of the x component of the spin polarization into the terminals.

The transverse components of the spin-polarization flow do oscillate with time since (see Appendix B)

$$\dot{\mathbf{M}}_L^{\rm tr}(t) = \frac{G}{G_0}\frac{\mathcal{F}(\Omega)}{2}\sin(2k_{so}d)[0, \sin(\Omega t), -\cos(\Omega t)]. \quad (17)$$

The sum of the two transverse spin components is directed along the vector $[0, \sin(\Omega t), -\cos(\Omega t)]$. Integration over time yields a transverse spin polarization $\mathbf{M}_L^{\rm tr}(t) = \int^t \dot{\mathbf{M}}_L^{\rm tr}(t')dt'$, which is parallel to the effective magnetic field, i.e., to $\hat{\mathbf{v}}(t)$, Eq. (12).

IV. ELLIPTICALLY ROTATING FIELD

The DC character of the flow of the longitudinal (x) component of the spin polarization is our main result. It is a remarkable consequence of the AC electric field responsible for the SOI and crucially depends on the fact that this electric field is rotating in the plane perpendicular to the weak link. To elucidate this point we allow for different amplitudes of the electric field components oscillating in the two transverse (y and z) directions. In that case the tunneling amplitude takes the form

$$W_{LR}(t)/W_0 = \cos[U(t)k_{so}d] + i\sin[U(t)k_{so}d]\boldsymbol{\sigma}\cdot\hat{\mathbf{u}}(t), \quad (18)$$

where

$$\hat{\mathbf{u}}(t) = \mathbf{U}(t)/U(t) \equiv [0, \cos(\Omega t), \gamma\sin(\Omega t)]/U(t) \quad (19)$$

and

$$U(t) = \sqrt{\cos^2(\Omega t) + \gamma^2\sin^2(\Omega t)}. \quad (20)$$

As seen, γ measures the deviation away from the circular polarization: $\gamma = 0$ corresponds to a linear-polarized electric field, while $\gamma = 1$ restores the circularly polarized field, Eq. (12).

Whereas a circularly polarized electric field implies single-photon absorption and emission processes [as expressed by the δ functions in Eq. (16)], the intricate time dependence [see Eq. (20)] of the noncircular polarization leads to an infinite Fourier series in powers of $\exp[in\Omega t]$ and, consequently, to an infinite series of δ functions expressing multiple-photon processes of emission and absorption. However, upon retaining only terms up to second order in $(k_{so}d)$ Eq. (18) becomes

$$W_{LR}(t)/W_0 \approx 1 - [U(t)(k_{so}d)]^2/2 + i(k_{so}d)\,\boldsymbol{\sigma}\cdot\mathbf{U}(t). \quad (21)$$

The spin part here, which determines $\dot{\mathbf{M}}_L(t)$, has the same form as in a similarly expanded Eq. (11), except that the coefficient of σ_z is multiplied by γ. Repeating the previous

calculation, this reproduces Eqs. (15) and (17), except that the x and z components of $\dot{\mathbf{M}}_L$ are now multiplied by γ. Therefore, in the longitudinal limit $\gamma = 0$ and for a small SOI there is no DC spin current, while the transverse spin current oscillates only in the $\hat{\mathbf{y}}$ direction.

V. DISCUSSION

An external magnetic field, whose orientation varies with time, prevents the spin of an electron from being a good quantum number and induces spin-flip transitions. Spin pumping of electrons in semiconductors by circularly polarized light [34] and spin currents generated by magnetization dynamics in conducting ferromagnets [35] are well-known consequences of this fact. These phenomena are, however, distinct from the effect discussed here. This is because a time-independent SOI, in contrast to a Zeeman coupling, preserves time-reversal symmetry and hence [12] does not affect electronic transport properties. Rather, a Rashba-type SOI generates an energy-independent Aharonov-Casher phase, which can affect electron transport only if time-reversal symmetry is broken in some other way. In our work this is achieved by assuming that the SOI is generated by a time-dependent (AC) electric field. If a constant-magnitude electric field rotates in the plane perpendicular to a one-dimensional wire, the DC spin current (spin-polarization flow) given by Eq. (15) is generated.

To elaborate on the physical reason for the generation of this DC spin current we note that semiclassically, the effect of the SOI (here restricted to act in only the weak link) can be viewed as a precession of the spin of the electrons during their passage through the link. When the SOI is due to an electric field that rotates in the plane perpendicular to the weak link, the direction of the spin-rotation axis, which is perpendicular to both the electric field and the direction of electron propagation, rotates in the same plane, and there is no spin component that can be chosen as an integral of motion. Since spin is not conserved in the weak link, excess spin is accumulated there. This is why the electron flow injected from the weak link into the left lead as well as the right lead carries net spin corresponding to a spin current through the leads generated in the weak link. A remarkable result of our calculation is that the total rate of spin generation in the link (the number of spins injected into the leads per unit time) does not depend on time if the electric field responsible for the SOI has a constant magnitude and rotates by a constant frequency.

In reality, the flow of the spin-polarized electrons injected from the junction into the adjacent parts of the terminals has a certain spatial dependence. For one-dimensional leads (in the absence of the SOI and magnetic fields), we expect the extra charge and spin polarization in the terminals to follow a classical trajectory with the Fermi velocity $v_{\rm F}$ in the leads, e.g., $M_{L,x}(r,t) = M_{L,x}(0, t - r/v_{\rm F})$ at a distance r from the edge of the junction, up to a certain length determined by the impurity scattering length in the terminal. The periodic rotation of the transverse spin components will translate into a periodic rotation in space. In higher dimensions, the ballistic electronic motion can be treated as in the theory of point-contact spectroscopy of metals, with the corresponding densities decaying as $(r_0/r)^{\xi}$, where r_0 characterizes the cross section of the junction and $\xi = 2$ ($\xi = 1$) in the ballistic (diffusive) transport regime. [36]

In the closed-circuit configuration [28] sketched in Fig. 1(a) the magnetization injected into the leads can be measured, e.g., by a properly positioned superconducting quantum interference device or by a magnetic-resonance force microscope. Alternatively, an open circuit [28] such as the one sketched in Fig. 1(b), where magnetization is accumulated in two terminals, can be used. Here low-dimensional contacts connect the weak link to terminals whose linear dimension significantly exceeds the cross section of the contacts so that the terminals can be thought of as reservoirs where injected polarized spins spend a significant time—much longer than the spin relaxation time—before they are reflected back to the weak link.

An estimate for the amount of magnetization accumulated in one of the terminals during a time interval of the order of the spin relaxation time τ_s will then be $(g\mu_B/2)\dot{M}_{L,x}\tau_s$. Using Eqs. (15) and (16) without any bias voltage, $\mu_L = \mu_R$, we find that in the small-Ω limit

$$\dot{M}_{L,x} = (\Omega/\pi)(G/G_0)\sin^2(k_{\rm so}d). \tag{22}$$

Consider now an SOI-active weak link in the form of an InAs nanowire and adopt the value $k_{\rm so} = 1/(100\,{\rm nm})$ measured by Scherübl *et al.* [37]. A wire length of $d = 100\,{\rm nm}$ would then give $k_{\rm so}d = 1$ and hence $\sin^2(k_{\rm so}d) \approx 1$. For $\Omega = 2\pi \times 20\,{\rm GHz}$ and using the typical value $G \sim 0.5G_0$ for the normal conductance of InAs nanowires [37–39], one then finds that $\dot{M}_{L,x} \approx 2 \times 10^{10}\ {\rm s}^{-1}$. Next, consider n-type bulk GaAs terminals [see Fig. 1(b)] moderately doped to give a low electron density of $1 \times 10^{16}\ {\rm cm}^{-3}$, for which spin relaxation times as long as $\tau_s = 100\,{\rm ns}$ have been measured at low temperatures [40]. Using the measured value $g = -0.45$ for the g factor of conduction electrons in bulk GaAs [41], we then arrive at the conclusion that spins corresponding to a magnetization of about 500 Bohr magnetons may accumulate in the terminals, which, if they were cubes with side lengths of $1\,\mu{\rm m}$, would contain $\sim$10 000 electrons.

As stated, we expect our approximation (3) to be valid when $\Omega \ll 1/\tau$, or, equivalently, when $\hbar\Omega \ll \Gamma$, where $\Gamma = \hbar/\tau$ is the level width in the wire. For this purpose we use the estimate $\Gamma = D\hbar v_{\rm F}/d$, where $D \sim G/G_0 = 0.5$ is the transparency of the barriers between the wire and the terminals and $v_{\rm F} = \ell_e e/(m^*\mu_e)$ is the Fermi velocity of electrons in the wire, here related to the electron mobility μ_e, the electron mean free path ℓ_e, and the effective mass $m^* = 0.023m$. Using the typical InAs nanowire values $\mu_e = 3000\ {\rm cm}^2/({\rm V\,s})$ and $\ell_e = 55\,{\rm nm}$ (taken from Ref. [39]), we find that $v_{\rm F} \approx 1 \times 10^8\,{\rm cm/s}$ and hence $\Gamma \approx 3\,{\rm meV}$. Since $\hbar\Omega \approx 0.1\,{\rm meV}$ for $\Omega = 2\pi \times 20\,{\rm GHz}$, we are indeed in the low-frequency regime.

In conclusion we have shown that a rotating electric field, acting on a weak link between two nonmagnetic metals, generates both a DC spin current and transverse spin components which rotate around the link, flowing into both metals. This is a simple device, with potential uses as a logic element in quantum data processing. Our estimates show that it can realistically be made with existing materials and technology.

ACKNOWLEDGMENTS

We thank J. Suh and C. Kim for fruitful discussions. This research was partially supported by the Israel Science Foundation (ISF), by the infrastructure program of the Israel Ministry of Science and Technology under Contract No. 3-11173, by the Pazy Foundation, by the Croatian Science Foundation, Project No. IP-2016-06-2289, and by the QuantiXLie Centre of Excellence, a project cofinanced by the Croatian government and the European Union through the European Regional Development Fund-the Competitiveness and Cohesion Operational Programme (Grant No. KK.01.1.1.01.0004). M.J., R.I.S., O.E.-W., A.A., and D.R. acknowledge the hospitality of the PCS at IBS, Daejeon, Korea, where part of this work was done. Work at the IBS was supported by IBS funding number (IBS-R024-D1).

APPENDIX A: DERIVATION OF PARTICLE AND SPIN CURRENTS IN THE MODEL JUNCTION

As explained in the main text, the tunnel junction is modeled by the Hamiltonian $\mathcal{H} = \mathcal{H}_{\rm leads} + \mathcal{H}_{\rm tun}(t)$, Eq. (4), in which $\mathcal{H}_{\rm leads}$, given by Eq. (5), describes the nonpolarized (free-electron) leads. Tunneling between the leads is described by the time- and spin-dependent Hamiltonian (1).

For nonpolarized leads, one finds

$$\begin{aligned}[R_L]_{\sigma\sigma'}(t) &\equiv \frac{d}{dt}\sum_k \langle c^\dagger_{k\sigma}(t)c_{k\sigma'}(t)\rangle \\ &= i\sum_{k,p}\sum_{\sigma_1}\Big\{[W^*_{LR}(t)]_{\sigma\sigma_1}\big\langle c^\dagger_{p\sigma_1}(t)c_{k\sigma'}(t)\big\rangle \\ &\quad - [W_{LR}(t)]_{\sigma'\sigma_1}\big\langle c^\dagger_{k\sigma}(t)c_{p\sigma_1}(t)\big\rangle\Big\}. \qquad \text{(A1)}\end{aligned}$$

The quantum averages in the first and second terms on the right-hand side of Eq. (A1) are calculated to lowest order in the tunneling (using units in which $\hbar = 1$)

$$\begin{aligned}\big\langle c^\dagger_{p\sigma_1}(t)c_{k\sigma'}(t)\big\rangle &= i\int_{-\infty}^{t} dt_1 e^{\eta t_1} e^{i(\epsilon_p-\epsilon_k)(t-t_1)} \\ &\quad\times [W_{LR}(t_1)]_{\sigma'\sigma_1}[f_L(\epsilon_k) - f_R(\epsilon_p)], \\ \langle c^\dagger_{k\sigma}(t)c_{p\sigma_1}(t)\rangle &= i\int_{-\infty}^{t} dt_1 e^{\eta t_1} e^{i(\epsilon_k-\epsilon_p)(t-t_1)} \\ &\quad\times [W^*_{LR}(t_1)]_{\sigma\sigma_1}[f_R(\epsilon_p) - f_L(\epsilon_k)], \qquad \text{(A2)}\end{aligned}$$

where $\eta \to 0^+$. Inserting Eqs. (A2) into Eq. (A1) gives

$$\begin{aligned}[R_L]_{\sigma\sigma'}(t) &= \sum_{k,p}[f_R(\epsilon_p) - f_L(\epsilon_k)]\int_{-\infty}^{t} dt_1 e^{\eta t_1} \\ &\quad\times \{e^{i(\epsilon_k-\epsilon_p)(t-t_1)}[W_{LR}(t)W^\dagger_{LR}(t_1)]_{\sigma'\sigma} \\ &\quad + e^{i(\epsilon_p-\epsilon_k)(t-t_1)}[W_{LR}(t_1)W^\dagger_{LR}(t)]_{\sigma'\sigma}\}. \qquad \text{(A3)}\end{aligned}$$

APPENDIX B: EXPLICIT EXPRESSIONS FOR I_L AND $\dot{\mathbf{M}}_L$ FOR A CIRCULARLY POLARIZED FIELD

As discussed in the main text, the time and spin dependence of the tunneling amplitude $W_{LR}(t)$ results from the Aharonov-Casher phase operator, in conjunction with an oscillating electric field. For a circularly polarized electric field the tunneling amplitude is given by Eq. (11), and the vector $\hat{\mathbf{v}}(t)$ is given by Eq. (12). This yields Eq. (13).

It follows that the trace of the matrix on the right-hand side, which appears in the expression for the particle current (7), is

$$\begin{aligned}&\mathrm{Tr}[W_{LR}(t)W^\dagger_{LR}(t_1)] \\ &\quad = 2|W_0|^2\big\{\cos^2(k_{\rm so}d) + \sin^2(k_{\rm so}d)\cos[\Omega(t-t_1)]\big\}. \qquad \text{(B1)}\end{aligned}$$

As it depends only upon the times' difference $t - t_1$, the particle current through the junction does not vary with t. The same type of time dependence appears in the σ_x component of the product in Eq. (13), which can be written as

$$\mathrm{Tr}[\sigma_x W_{LR}(t)W^\dagger_{LR}(t_1)] = -2i|W_0|^2\sin^2(k_{\rm so}d)\sin[\Omega(t-t_1)]. \qquad \text{(B2)}$$

As a result, the x component of the spin current $\dot{M}_{L,x}$ is also independent of time. On the other hand, the spin currents $\dot{M}_{L,y}$ and $\dot{M}_{L,z}$, are determined by

$$\begin{aligned}&\mathrm{Tr}[\sigma_y W_{LR}(t)W^\dagger_{LR}(t_1)] \\ &\quad = 2i|W_0|^2\cos(k_{\rm so}d)\sin(k_{\rm so}d)[\cos(\Omega t) - \cos(\Omega t_1)], \\ &\mathrm{Tr}[\sigma_z W_{LR}(t)W^\dagger_{LR}(t_1)] \\ &\quad = 2i|W_0|^2\cos(k_{\rm so}d)\sin(k_{\rm so}d)[\sin(\Omega t) - \sin(\Omega t_1)] \qquad \text{(B3)}\end{aligned}$$

and, consequently, are time dependent.

Using Eqs. (A3) and (B1) in conjunction with Eq. (7), one finds the particle current into the left lead,

$$\begin{aligned}I_L &= 2|W_0|^2\sum_{k,p}[f_R(\epsilon_p) - f_L(\epsilon_k)]\int_{-\infty}^{t} dt_1 e^{\eta t_1}(\cos^2(k_{\rm so}d) + \sin^2(k_{\rm so}d)\cos[\Omega(t-t_1)])(e^{i(\epsilon_k-\epsilon_p)(t-t_1)} + e^{i(\epsilon_p-\epsilon_k)(t-t_1)}) \\ &= 4\pi|W_0|^2\sum_{k,p}[f_R(\epsilon_p) - f_L(\epsilon_k)]\left(\cos^2(k_{\rm so}d)\delta(\epsilon_k-\epsilon_p) + \frac{1}{2}\sin^2(k_{\rm so}d)[\delta(\epsilon_k-\epsilon_p+\Omega) + \delta(\epsilon_k-\epsilon_p-\Omega)]\right). \qquad \text{(B4)}\end{aligned}$$

To zeroth order in Ω the terms within the round brackets reduce to $\delta(\epsilon_k - \epsilon_p)$; hence, up to linear order in Ω the conductance is not affected by the spin-orbit coupling. The particle current into the right terminal is obtained from Eq. (B4) upon interchanging k with p and L with R. Hence, $I_R = -I_L$.

Equations (A3) and (B2) in conjunction with Eq. (8) give

$$\dot{M}_{L,x} = 2|W_0|^2 \sin^2(k_{\rm so}d) \sum_{k,p} [f_R(\epsilon_p) - f_L(\epsilon_k)] \int_{-\infty}^{t} dt_1 e^{\eta t_1} (-ie^{i(\epsilon_k-\epsilon_p)(t-t_1)} + ie^{i(\epsilon_p-\epsilon_k)(t-t_1)}) \sin[(\Omega(t-t_1)]$$

$$= 2\pi |W_0|^2 \sin^2(k_{\rm so}d) \sum_{k,p} [f_R(\epsilon_p) - f_L(\epsilon_k)](\delta(\epsilon_k - \epsilon_p + \Omega) - \delta(\epsilon_k - \epsilon_p - \Omega)). \tag{B5}$$

The terms in the round brackets give a contribution of order Ω to $\dot{M}_{L,x}$. The corresponding spin current in the right reservoir $\dot{M}_{R,x}$ is obtained from Eq. (B5) by interchanging k with p and L with R; as seen, it has the same sign as that of $\dot{M}_{L,x}$.

From the first of Eqs. (B3) in conjunction with Eqs. (8) and (A3) it follows that

$$\dot{M}_{L,y} = 2|W_0|^2 \cos(k_{\rm so}d) \sin(k_{\rm so}d) \sum_{k,p} [f_R(\epsilon_p) - f_L(\epsilon_k)] \int_{-\infty}^{t} dt_1 e^{\eta t_1} (ie^{i(\epsilon_k-\epsilon_p)(t-t_1)} - ie^{i(\epsilon_p-\epsilon_k)(t-t_1)})[\cos(\Omega t) - \cos(\Omega t_1)]. \tag{B6}$$

As

$$\cos(\Omega t) - \cos(\Omega t_1) = \cos(\Omega t) - \{\cos(\Omega t)\cos[\Omega(t-t_1)] + \sin(\Omega t)\sin[\Omega(t-t_1)]\}, \tag{B7}$$

we find

$$\dot{M}_{L,y} = -2|W_0|^2 \sin(2k_{\rm so}d) \sum_{k,p} [f_R(\epsilon_p) - f_L(\epsilon_k)] \Bigg\{ \cos(\Omega t) \Bigg(\frac{\mathcal{P}}{\epsilon_k - \epsilon_p} - \frac{1}{2} \Bigg[\frac{\mathcal{P}}{\epsilon_k - \epsilon_p + \Omega} + \frac{\mathcal{P}}{\epsilon_k - \epsilon_p - \Omega} \Bigg] \Bigg)$$

$$+ (\pi/2) \sin(\Omega t)[\delta(\epsilon_k - \epsilon_p + \Omega) - \delta(\epsilon_k - \epsilon_p - \Omega)] \Bigg\}, \tag{B8}$$

where $\mathcal{P}$ indicates the principal part. Likewise,

$$\dot{M}_{L,z} = 2|W_0|^2 \cos(k_{\rm so}d) \sin(k_{\rm so}d) \sum_{k,p} [f_R(\epsilon_p) - f_L(\epsilon_k)] \int_{-\infty}^{t} dt_1 e^{\eta t_1} (ie^{i(\epsilon_k-\epsilon_p)(t-t_1)} - ie^{i(\epsilon_p-\epsilon_k)(t-t_1)})[\sin(\Omega t) - \sin(\Omega t_1)], \tag{B9}$$

with

$$\sin(\Omega t) - \sin(\Omega t_1) = \sin(\Omega t) - \{\sin(\Omega t)\cos[\Omega(t-t_1)] - \cos(\Omega t)\sin[\Omega(t-t_1)]\}, \tag{B10}$$

leads to

$$\dot{M}_{L,z} = -2|W_0|^2 \sin(2k_{\rm so}d) \sum_{k,p} [f_R(\epsilon_p) - f_L(\epsilon_k)] \Bigg\{ \sin(\Omega t) \Bigg(\frac{\mathcal{P}}{\epsilon_k - \epsilon_p} - \frac{1}{2} \Bigg[\frac{\mathcal{P}}{\epsilon_k - \epsilon_p + \Omega} + \frac{\mathcal{P}}{\epsilon_k - \epsilon_p - \Omega} \Bigg] \Bigg)$$

$$- (\pi/2) \cos(\Omega t)(\delta(\epsilon_k - \epsilon_p + \Omega) - \delta(\epsilon_k - \epsilon_p - \Omega)) \Bigg\}. \tag{B11}$$

The principal parts in Eqs. (B8) and (B11) are of order Ω^2 and hence can be neglected in the small-Ω limit. The remaining terms, which are of order Ω, rotate in the y-z plane, along the vector $[0, \sin(\Omega t), -\cos(\Omega t)]$. Remarkably, this vector corresponds to a transverse magnetization parallel to the effective magnetic field, which is directed along $\hat{\mathbf{v}}(t)$, Eq. (12).

[1] S. A. Wolf, D. D. Awschalom, R. A. Buhrman, J. M. Daughton, S. von Molnár, M. L. Roukes, A. Y. Chtchelkanova, and D. M. Treger, Spintronics: A spin-based electronics vision for the future, Science **294**, 1488 (2001).

[2] I. Žutić, J. Fabian, and S. Das Sarma, Spintronics: Fundamentals and applications, Rev. Mod. Phys. **76**, 323 (2004).

[3] J. Kim, A. Paul, P. A. Crowell, S. J. Koester, S. S. Sapatnekar, J. Wang, and C. H. Kim, Spin-based computing: Device concepts, current status, and a case study on a high-performance microprocessor, Proc. IEEE **103**, 106 (2015).

[4] M. Kohda and J. Nitta, Enhancement of spin-orbit interaction and the effect of interface diffusion in quaternary InGaAsP/InGaAs heterostructures, Phys. Rev. B **81**, 115118 (2010).

[5] R. Winkler, *Spin-Orbit Coupling Effects in Two-Dimensional Electron and Hole Systems* (Springer, Berlin, 2003).

[6] A. Manchon, H. C. Koo, J. Nitta, S. M. Frolov, and R. A. Duine, New perspectives for rashba spin-orbit coupling, Nat. Mater. **14**, 871 (2015).

[7] E. I. Rashba, Properties of semiconductors with an extremum loop. 1. Cyclotron and combinational resonance in a magnetic

field perpendicular to the plane of the loop, Fiz. Tverd. Tela (Leningrad) **2**, 1224 (1960) [Sov. Phys. Solid State **2**, 1109 (1960)]; Yu. A. Bychkov and E. I. Rashba, Oscillatory effects and the magnetic susceptibility of carriers in inversion layers, J. Phys. C **17**, 6039 (1984).

[8] J. Nitta, T. Akazaki, H. Takayanagi, and T. Enoki, Gate Control of Spin-Orbit Interaction in an Inverted $In_{0.53}Ga_{0.47}As/In_{0.52}Al_{0.48}As$ Heterostructure, Phys. Rev. Lett. **78**, 1335 (1997).

[9] Y. Sato, T. Kita, S. Gozu, and S. Yamada, Large spontaneous spin splitting in gate-controlled two-dimensional electron gases at normal $In_{0.75}Ga_{0.25}As/In_{0.75}Al_{0.25}As$ heterojunctions, J. Appl. Phys. **89**, 8017 (2001).

[10] A. J. A. Beukman, F. K. de Vries, J. van Veen, R. Skolasinski, M. Wimmer, F. Qu, D. T. de Vries, B. M. Nguyen, W. Yi, A. A. Kiselev, M. Sokolich, M. J. Manfra, F. Nichele, C. M. Marcus, and L. P. Kouwenhoven, Spin-orbit interaction in a dual gated InAs/GaSb quantum well, Phys. Rev. B **96**, 241401(R) (2017).

[11] Other types of SOI, e.g., the Dresselhaus SOI [G. Dresselhaus, Spin-Orbit Coupling Effects in Zinc Blende Structures, Phys. Rev. **100**, 580 (1955)]; or those resulting from strains in the wire [M. S. Rudner and E. I. Rashba, Spin relaxation due to deflection coupling in nanotube quantum dots, Phys. Rev. B **81**, 125426 (2010); K. Flensberg and C. M. Marcus, Bends in nanotubes allow electric spin control and coupling, *ibid.* **81**, 195418 (2010); G. A. Steele, F. Pei, E. A. Laird, J. M. Jol, H. B. Meerwaldt, and L. P. Kouwenhoven, Large spin-orbit coupling in carbon nanotubes, Nat. Commun. **4**, 1573 (2013)], yield similar effects, with other directions of the effective SOI magnetic field around which the spins rotate.

[12] J. H. Bardarson, A proof of the Kramers degeneracy of transmission eigenvalues from antisymmetry of the scattering matrix, J. Phys. A **41**, 405203 (2008).

[13] A. G. Aronov and Y. B. Lyanda-Geller, Spin-Orbit Berry Phase in Conducting Rings, Phys. Rev. Lett. **70**, 343 (1993).

[14] A. Aharony, Y. Tokura, G. Z. Cohen, O. Entin-Wohlman, and S. Katsumoto, Filtering and analyzing mobile qubit information via Rashba-Dresselhaus-Aharonov-Bohm interferometers, Phys. Rev. B **84**, 035323 (2011) and references therein.

[15] H. Saarikoski, A. A. Reynoso, J. P. Baltanás, D. Frustaglia, and J. Nitta, Spin interferometry in anisotropic spin-orbit fields, Phys. Rev. B **97**, 125423 (2018); F. Nagasawa, A. A. Reynoso, J. P. Baltanás, D. Frustaglia, H. Saarikoski, and J. Nitta, Gate-controlled anisotropy in Aharonov-Casher spin interference: Signatures of Dresselhaus spin-orbit inversion and spin phases, *ibid.* **98**, 245301 (2018).

[16] P. M. Shmakov, A. P. Dmitriev, and V. Yu. Kachorovskii, High-temperature Aharonov-Bohm-Casher interferometer, Phys. Rev. B **85**, 075422 (2012); Aharonov-Bohm conductance of a disordered single-channel quantum ring, *ibid.* **87**, 235417 (2013).

[17] F. Nagasawa, J. Takagi, Y. Kunihashi, M. Kohda, and J. Nitta, Experimental Demonstration of Spin Geometric Phase: Radius Dependence of Time-Reversal Aharonov-Casher Oscillations, Phys. Rev. Lett. **108**, 086801 (2012).

[18] S. Datta and B. Das, Electronic analog of the electro-optic modulator, Appl. Phys. Lett. **56**, 665 (1990).

[19] A. Aharony, O. Entin-Wohlman, K. Sarkar, R. I. Shekhter, and M. Jonson, Effects of different lead magnetizations on the Datta-Das spin field-effect transistor, J. Phys. Chem. C **123**, 11094 (2019), and references therein.

[20] S. K. Watson, R. M. Potok, C. M. Marcus, and V. Umansky, Experimental Realization of a Quantum Spin Pump, Phys. Rev. Lett. **91**, 258301 (2003).

[21] B. Wang, J. Wang, and H. Guo, Quantum spin field effect transistor, Phys. Rev. B **67**, 092408 (2003).

[22] J. Splettstoesser, M. Governale, and J. König, Adiabatic charge and spin pumping through quantum dots with ferromagnetic leads, Phys. Rev. B **77**, 195320 (2008).

[23] P. Sharma and P. W. Brouwer, Mesoscopic Effects in Adiabatic Spin Pumping, Phys. Rev. Lett. **91**, 166801 (2003).

[24] M. Governale, F. Taddei, and R. Fazio, Pumping spin with electrical fields, Phys. Rev. B **68**, 155324 (2003).

[25] Y. Avishai, D. Cohen, and N. Nagaosa, Purely Electric Spin Pumping in One Dimension, Phys. Rev. Lett. **104**, 196601 (2010).

[26] Alternatively, the fields can be generated by a single back gate and two other gates placed very close to the sides of the wire as in Ref. [37].

[27] M. Jonson, R. I. Shekhter, O. Entin-Wohlman, A. Aharony, H. C. Park, and D. Radić, Mechanically driven spin-orbit-active weak links, Fiz. Niz. Temp. **44**, 1577 (2018) [Low Temp. Phys. **44**, 1228 (2018)].

[28] In a closed circuit, the two terminals are connected to each other via a voltage source (a battery), which generates a bias voltage, causing the current flow through the circuit. When there is no bias voltage, the two terminals can also be grounded. In an open circuit, the weak-link device and the terminals are electrically isolated from the environment. The term "open/closed circuit" (in electrical engineering) should not be confused with "open/closed system" in physics: the "open circuit" corresponds to the "closed system" and vice versa.

[29] The final results are expressed as traces over the σ's, and therefore, they do not depend on the quantization axes, which define the indices σ, σ'.

[30] Y. Aharonov and A. Casher, Topological Quantum Effects for Neutral Particles, Phys. Rev. Lett. **53**, 319 (1984).

[31] Y. Meir, Y. Gefen, and O. Entin-Wohlman, Universal Effects of Spin-Orbit Scattering in Mesoscopic Systems, Phys. Rev. Lett. **63**, 798 (1989); Y. Oreg and O. Entin-Wohlman, Transmissions through low-dimensional mesoscopic systems subject to spin-orbit scattering, Phys. Rev. B **46**, 2393 (1992).

[32] See Ref. [27]; see also A. Aharony, O. Entin-Wohlman, M. Jonson, and R. I. Shekhter, Electric and magnetic gating of Rashba-active weak links, Phys. Rev. B **97**, 220404(R) (2018), and Ref. [19].

[33] If the densities of states in the terminals are energy dependent (and equal), $\mathcal{N}_L(\epsilon) = \mathcal{N}_R(\epsilon) = \mathcal{N}(\epsilon)$, G in Eq. (14) should be multiplied by $\{1 + \sin^2(k_{so}d)[\mathcal{N}(\epsilon_F + \Omega) + \mathcal{N}(\epsilon_F - \Omega) - 2\mathcal{N}(\epsilon_F)]/[2\mathcal{N}(\epsilon_F)]\}$. Hence, there is a small SOI effect on the particle current of order $(\Omega/\epsilon_F)^2$.

[34] G. V. Astakhov, M. M. Glazov, D. R. Yakovlev, E. A. Zhukov, W. Ossau, L. W. Molenkamp, and M. Bayer, Time-resolved and continuous-wave optical spin pumping of semiconductor quantum wells, Semicond. Sci. Technol. **23**, 114001 (2008).

[35] Y. Tserkovnyak, A. Brataas, G. E. W. Bauer, and B. I. Halperin, Nonlocal magnetization dynamics in ferromagnetic heterostructures, Rev. Mod. Phys. **77**, 1375 (2005).

[36] I. O. Kulik, R. I. Shekhter, and A. G. Shkorbatov, Point contact spectroscopy of electron-phonon coupling in metals with a small electron mean free path, Zh. Eksp. Teor. Fiz. **81**, 2126 (1981) [Sov. Phys. JETP **54**, 1130 (1981)], Eqs. (2.11), (2.12), and (3.3)–(3.5); R. I. Shekhter and I. O. Kulik, Phonon spectroscopy in heterocontacts, Fiz. Nizk. Temp. **9**, 46 (1983) [Sov. J. Low Temp. Phys. **9**, 22 (1983)], Introduction and Sec. 1.

[37] Z. Scherübl, G. Fülöp, M. H. Madsen, J. Nygard, and S. Csonka, Electrical tuning of Rashba spin-orbit interaction in multi-gated InAs nanowires, Phys. Rev. B **94**, 035444 (2016).

[38] S. Chuang, Q. Gao, R. Kapadia, A. C. Ford, J. Guo, and A. Javey, Ballistic InAs nanowire transistors, Nano Lett. **13**, 555 (2012).

[39] S. A. Dayeh, Electron transport in indium arsenide nanowires, Semicond. Sci. Technol. **25**, 024004 (2010).

[40] J. M. Kikawa and D. D. Awschalom, Resonant Spin Amplification in *n*-Type GaAs, Phys. Rev. Lett. **80**, 4313 (1998).

[41] W. Zawadzki, P. Pfeffer, R. Bratschitsch, Z. Chen, S. T. Cundiff, B. N. Murdin, and C. R. Pidgeon, Temperature dependence of the electron spin *g* factor in GaAs, Phys. Rev. B **78**, 245203 (2008).